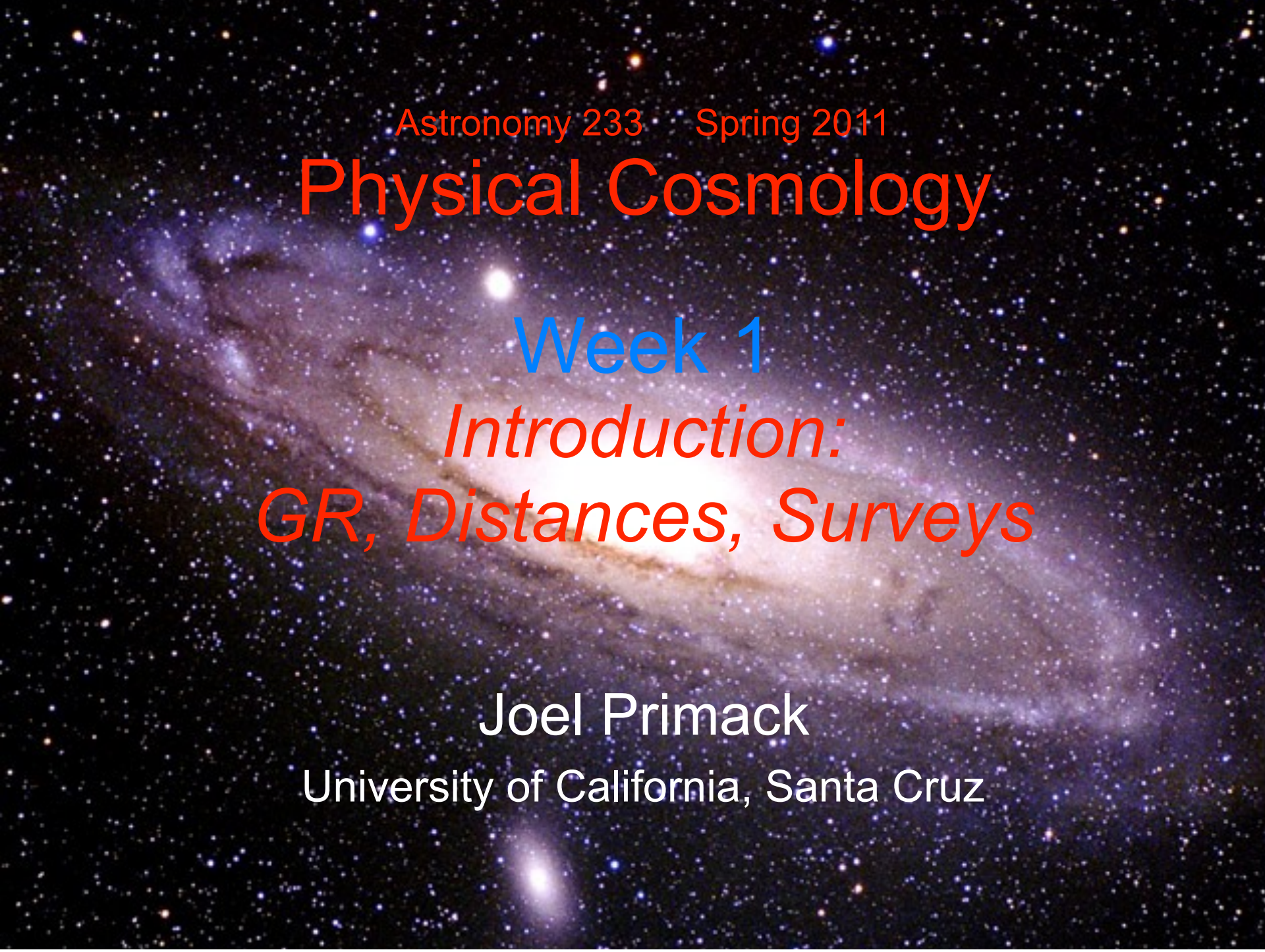
Astronomy 233 Spring 2011
Physical Cosmology
Week 1
Introduction:
GR, Distances, Surveys
Joel Primack
University of California, Santa Cruz

Modern Cosmology

A series of major discoveries has laid a lasting foundation for cosmology. Einstein's general relativity (1916) provided the conceptual foundation for the modern picture. Then Hubble discovered that "spiral nebulae" are large galaxies like our own Milky Way (1922), and that distant galaxies are receding from the Milky Way with a speed proportional to their distance (1929), which means that we live in an expanding universe. The discovery of the cosmic background radiation (1965) showed that the universe began in a very dense, hot, and homogeneous state: the Big Bang. This was confirmed by the discovery that the cosmic background radiation has exactly the same spectrum as heat radiation (1989), and the measured abundances of the light elements agree with the predictions of Big Bang theory if the abundance of ordinary matter is about 4% of critical density. Most of the matter in the universe is invisible particles which move very sluggishly in the early universe ("Cold Dark Matter"). Most of the energy density is mysterious dark energy.

Experimental and Historical Sciences

both make predictions about new knowledge, whether from experiments or from the past

Historical Explanation Is Always Inferential

Our age cannot look back to earlier things
Except where reasoning reveals their traces Lucretius

Patterns of Explanation Are the Same in the Historical Sciences as in the Experimental Sciences

Specific conditions + General laws ⇒ Particular event

In history as anywhere else in empirical science, the explanation of a phenomenon consists in subsuming it under general empirical laws; and the criterion of its soundness is … exclusively whether it rests on empirically well confirmed assumptions concerning initial conditions and general laws.

C.G. Hempel, *Aspects of Scientific Explanation* (1965), p. 240.

Successful Predictions of the Big Bang

First Prediction	First Confirmation
Expansion of the Universe	
Friedmann 1922, Lemaitre 1927 based on Einstein 1916	Hubble 1929
Cosmic Background Radiation	
Existence of CBR Gamow, Alpher, Hermann 1948	Penzias & Wilson 1965
CBR Thermal Spectrum Peebles 1966	COBE 1989
CBR Fluctuation Amplitude Cold Dark Matter theory 1984	COBE 1992
CBR Acoustic Peak	BOOMERANG 2000 MAXIMA 2000
Light Element Abundances	
Peebles 1966, Wagoner 1967	D/H Tytler et al. 1997

Three Pillars of the Big Bang

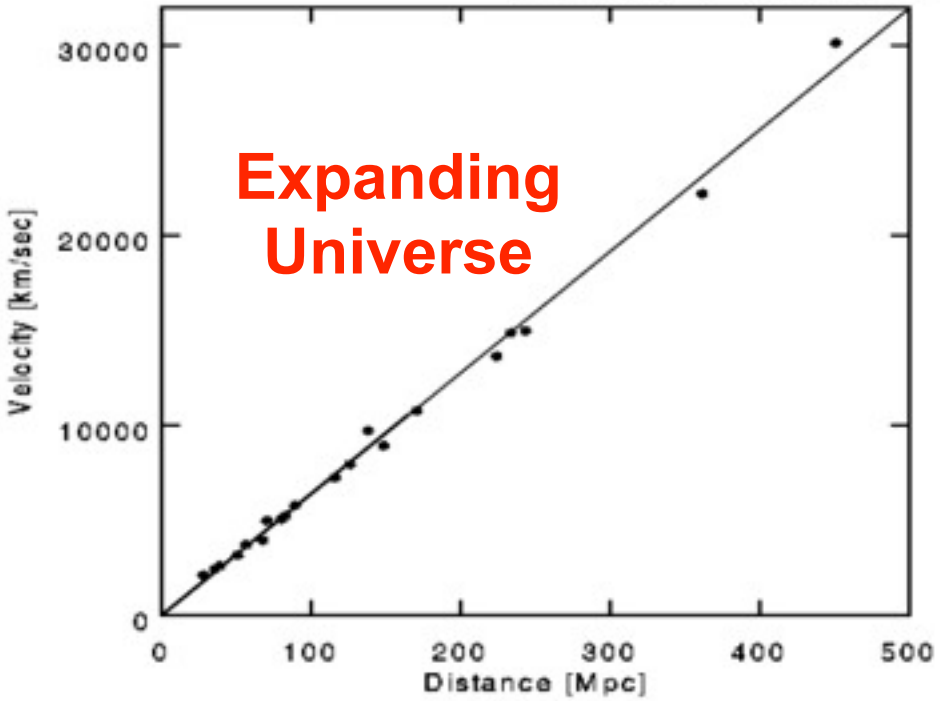

A modern illustration of Hubble's Law, displaying the increase of recession speed of galaxies growing in direct proportion to their distance.

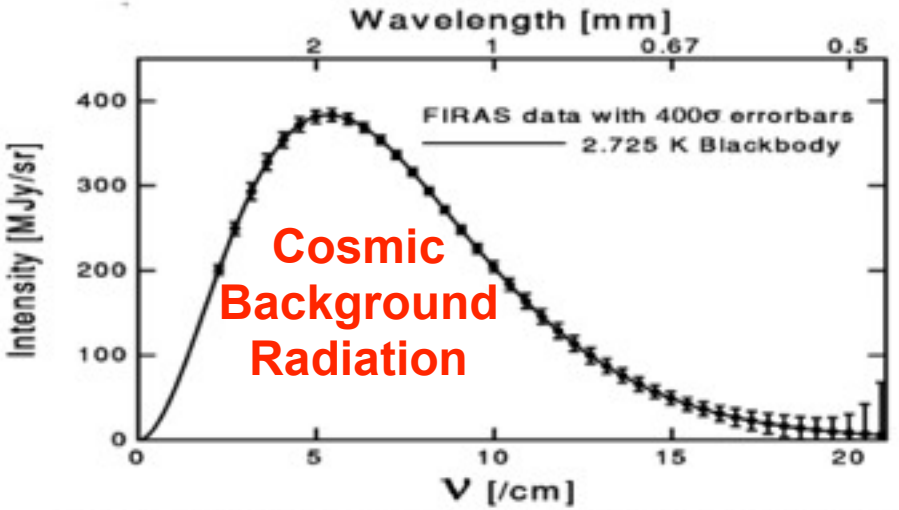

The variation of the intensity of the microwave background radiation with its frequency, as observed by the COBE satellite from above the Earth's atmosphere. The observations (boxes) display a perfect fit with the (solid) curve expected from pure heat radiation with a temperature of 2.73°K.

Big Bang Nucleosynthesis

The detailed production of the lightest elements out of protons and neutrons during the first three minutes of the universe's history. The nuclear reactions occur rapidly when the temperature falls below a billion degrees Kelvin. Subsequently, the reactions are shut down, because of the rapidly falling temperature and density of matter in the expanding universe.

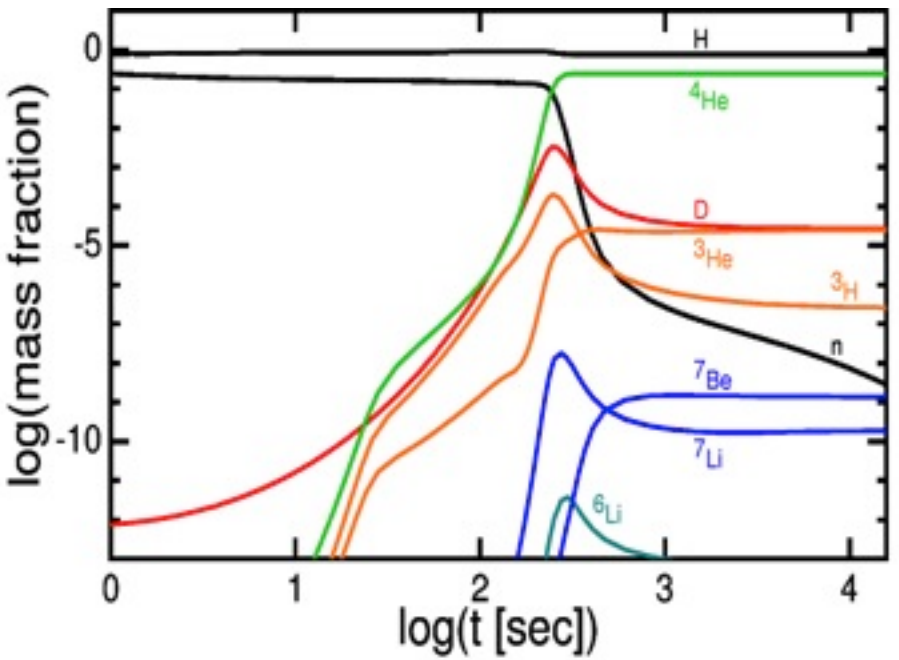

Caution: ^{7}Li may now be discordant

Mon. Not. R. astr. Soc. (1991) 251, 128-136

Dynamical effects of the cosmological constant

Ofer Lahav,[1] Per B. Lilje,[2] Joel R. Primack[3] and Martin J. Rees[1]

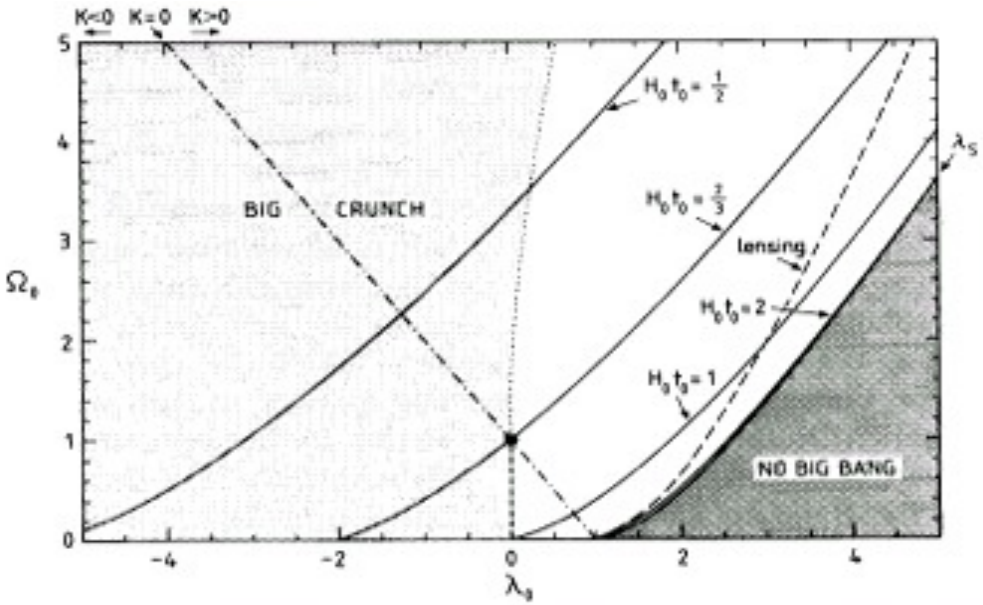

Figure 1. The phase-space of the density parameter Ω_0 and the cosmological constant $\lambda_0 \equiv \Lambda/(3H_0^2)$ with various fundamental constraints. The dashed-dotted line indicates an inflationary (i.e. flat) universe. Note that some open models will have a Big Crunch, while some closed models will expand forever. The solid lines show 4 values for the age of the universe H_0t_0, and the dashed line is the constraint of Gott *et al.* (1989) from a normally lensed quasar at $z = 3.27$. The boundary (λ_s) of the shaded 'No Big Bang' region corresponds to a coasting phase in the past, while the boundary of the 'Big Crunch' (for $\Omega_0 > 1$) region corresponds to a coasting phase in the future. We see that the permitted range in the $(\lambda_0 - \Omega_0)$ phase-space is fairly small, but allows values different from the popular point $(\Omega_0 = 1, \lambda_0 = 0)$.

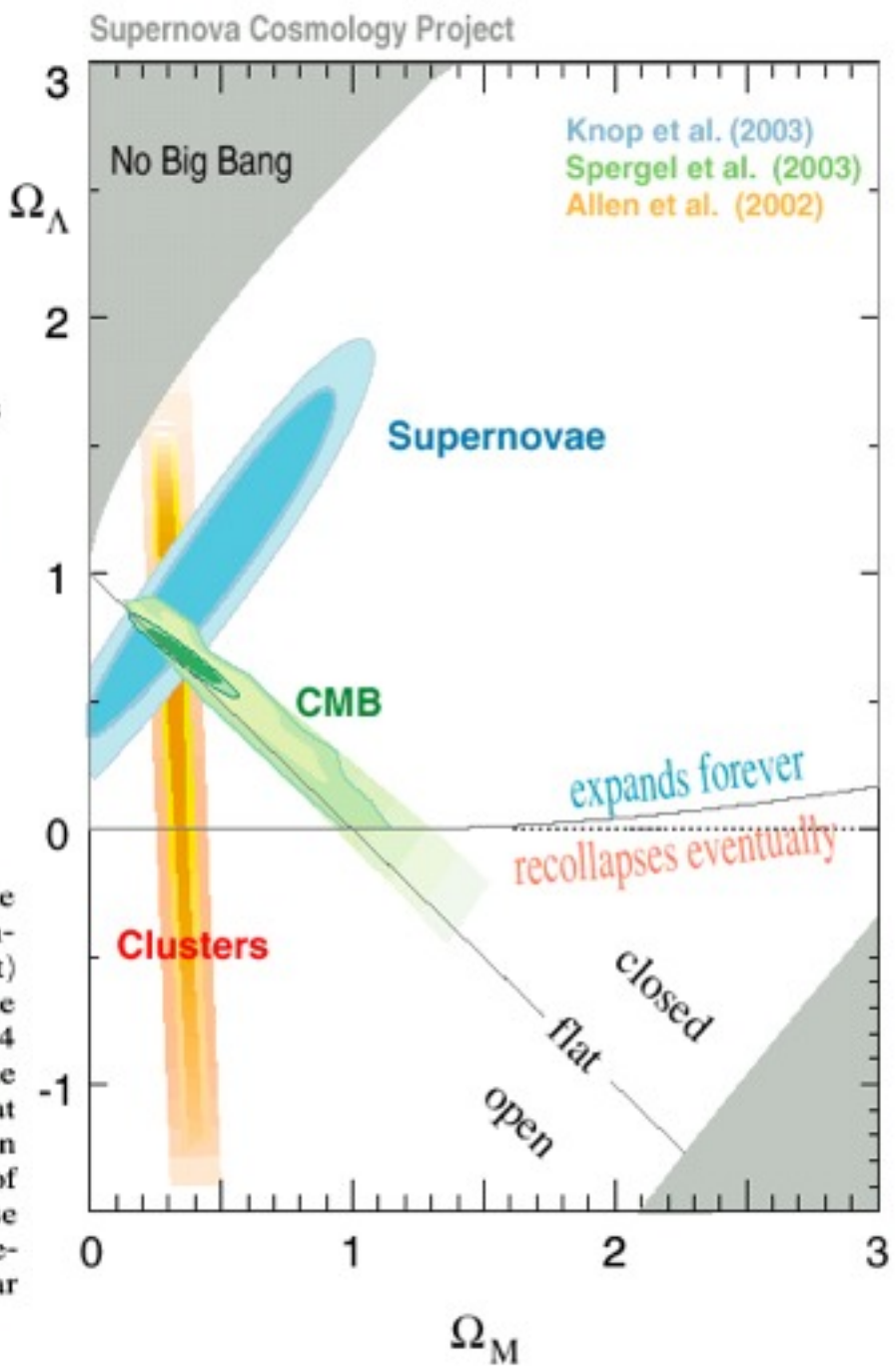

General Relativity and Cosmology

GR: MATTER TELLS SPACE HOW TO CURVE

$$R^{\mu\nu} - \tfrac{1}{2}Rg^{\mu\nu} = 8\pi G T^{\mu\nu} + \Lambda g^{\mu\nu}$$

CURVED SPACE TELLS MATTER HOW TO MOVE

$$\frac{du^{\mu}}{ds} + \Gamma^{\mu}{}_{\alpha\beta}\, u^{\alpha} u^{\beta} = 0$$

Cosmological Principle: on large scales, space is uniform and isotropic. COBE-Copernicus Theorem: If all observers observe a nearly-isotropic Cosmic Background Radiation (CBR), then the universe is locally nearly homogeneous and isotropic – i.e., is approximately described by the Friedmann-Robertson-Walker metric

$$ds^2 = dt^2 - a^2(t)\,[dr^2\,(1 - kr^2)^{-1} + r^2\, d\Omega^2]$$

with curvature constant $k = -1, 0,$ or $+1$. Substituting this metric into the Einstein equation at left above, we get the Friedmann eq.

Friedmann-Robertson-Walker Framework (homogeneous, isotropic universe)

FRW E(00) $\frac{\dot{a}^2}{a^2} = \frac{8\pi}{3}G\rho - \frac{k}{a^2} + \frac{\Lambda}{3}$ ← Friedmann equation

FRW E(ii) $\frac{2\ddot{a}}{a} + \frac{\dot{a}^2}{a^2} = -8\pi G p - \frac{k}{a^2} + \Lambda$

$H_0 \equiv 100h\,\mathrm{km\,s^{-1}}$ Mpc^{-1}
$\equiv 70h_{70}\,\mathrm{km\,s^{-1}}$ Mpc^{-1}

$$\frac{E(00)}{H_0^2} \Rightarrow 1 = \Omega_0 - \frac{k}{H_0^2} + \Omega_\Lambda \text{ with } H \equiv \frac{\dot{a}}{a},\ a_0 \equiv 1,\ \Omega_0 \equiv \frac{\rho_0}{\rho_c}, \Omega_\Lambda \equiv \frac{\Lambda}{3H_0^2},$$

$$\rho_{c,0} \equiv \frac{3H_0^2}{8\pi G} = 1.36 \times 10^{11} h_{70}^2 M_\odot \mathrm{Mpc}^{-3}$$

$$E(ii) - E(00) \Rightarrow \frac{2\ddot{a}}{a} = -\frac{8\pi}{3}G\rho - 8\pi G p + \frac{2}{3}\Lambda$$

$$\text{Divide by } 2E(00) \Rightarrow \quad q_0 \equiv -\left(\frac{\ddot{a}}{a}\frac{a^2}{\dot{a}^2}\right)_0 = \frac{\Omega_0}{2} - \Omega_\Lambda$$

$$E(00) \Rightarrow t_0 = \int_0^1 \frac{da}{a}\left[\frac{8\pi}{3}G\rho - \frac{k}{a^2} + \frac{\Lambda}{3}\right]^{-\frac{1}{2}} = H_0^{-1}\int_0^1 \frac{da}{a}\left[\frac{\Omega_0}{a^3} - \frac{k}{H_0^2 a^2} + \Omega_\Lambda\right]^{-\frac{1}{2}}$$

$t_0 = H_0^{-1} f(\Omega_0, \Omega_\Lambda)$ $\quad H_0^{-1} = 9.78h^{-1}\mathrm{Gyr}$ $\quad f(1,0) = \frac{2}{3}$
$f(0,0) = 1$
$f(0,1) = \infty$

$= 13.97\ \mathrm{h_{70}}^{-1}$ Gyr $\quad f(0.3, 0.7) = 0.964$

$$[E(00)a^3]' \text{ vs. } E(ii) \Rightarrow \quad \frac{\partial}{\partial a}(\rho a^3) = -3pa^2 \text{ (“continuity”)}$$

Given eq. of state $p = p(\rho)$, integrate to determine $\rho(a)$,
integrate $E(00)$ to determine $a(t)$

Matter: $p = 0 \Rightarrow \rho = \rho_0 a^{-3}$ (assumed above in q_0, t_0 eqs.)

Radiation: $p = \frac{\rho}{3},\ k = 0 \Rightarrow \rho \propto a^{-4}$

Measuring Distances in the Universe

Primary Distance Indicators

Trigonometric parallax

α Centauri 1.35 pc - first measured by Thomas Henderson 1832

61 Cygni 3.48 pc - by Friedrich Wilhelm Bessel in 1838

Only a few stars to < 30 pc, until the Hipparcos satellite 1997 measured distances of 118,000 stars to about 100 pc, about 20,000 stars to <10%.

Proper motions

Moving cluster method

Mainly for the Hyades, at about 100 pc. Now supplanted by Hipparcos.

Distance to Cepheid ζ Geminorum = 336 ± 44 pc

Using Doppler to measure change of diameter, and interferometry to measure change of angular diameter.

Similar methods for Type II SN, for stars in orbit about the Sagittarius A* SMBH (gives distance 8.0 ± 0.4 kpc to Galactic Center), for radio maser in NGC 4258 (7.2 ± 0.5 Mpc), etc.

Apparent Luminosity of various types of stars

$L = 10^{-2M/5}\ 3.02\times10^{35}$ erg sec^{-1} where $M_{vis} = +4.82$ for the sun

Apparent luminosity $\ell = L\,(4\pi d^2)^{-1}$ for nearby objects,
related to apparent magnitude m by $\ell = 10^{-2m/5}\ (2.52\times10^{-5}$ erg cm^{-2} s$^{-1})$

Distance modulus m - M related to distance by $d = 10^{1\ +\ (m\ -\ M)/5}$ pc

Main sequence stars were calibrated by Hipparchos distances
and the Hubble Space Telescope Fine Guidance Sensor
Red clump (He burning) stars.
RR Lyrae Stars - variables with periods 0.2 - 0.8 days
Eclipsing binaries - v from Doppler, ellipticity from v(t), radius of primary from duration of eclipse, T from spectrum, gives $L = \sigma T^4 \pi R^2$
Cepheid variables - bright variable stars with periods 2 - 45 days

Henrietta Swan Leavitt in 1912 discovered the Cepheid period-luminosity relation in the SMC, now derived mainly from the LMC. This was the basis for Hubble's 1923 finding that M32 is far outside the Milky Way. Best value today for the LMC distance modulus m - M = 18.50 (see Weinberg, *Cosmology*, p. 25), or $d_{LMC} = 50.1$ kpc.

Hertzsprung-Russell Diagram

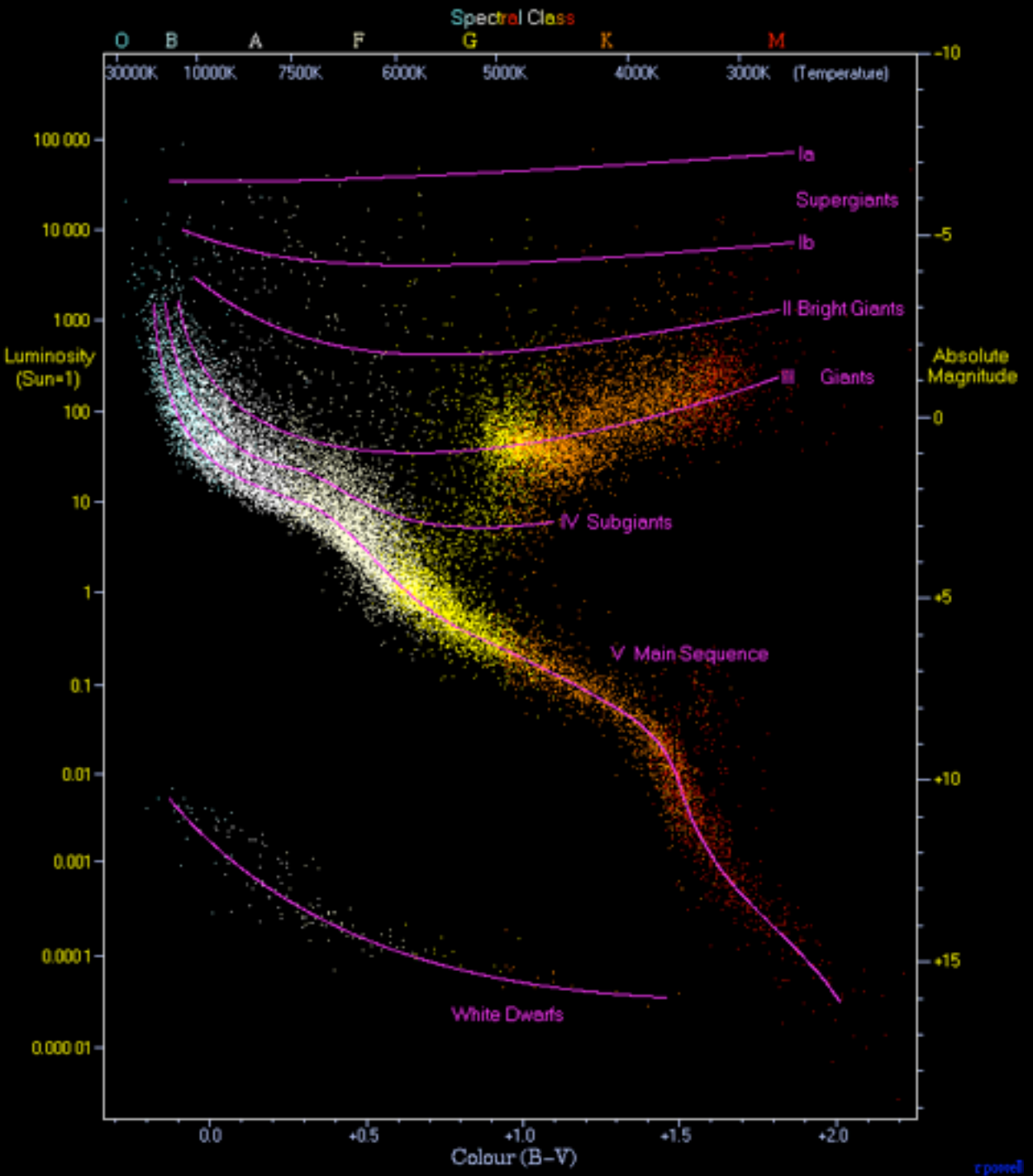

Hertzsprung-Russell Diagram

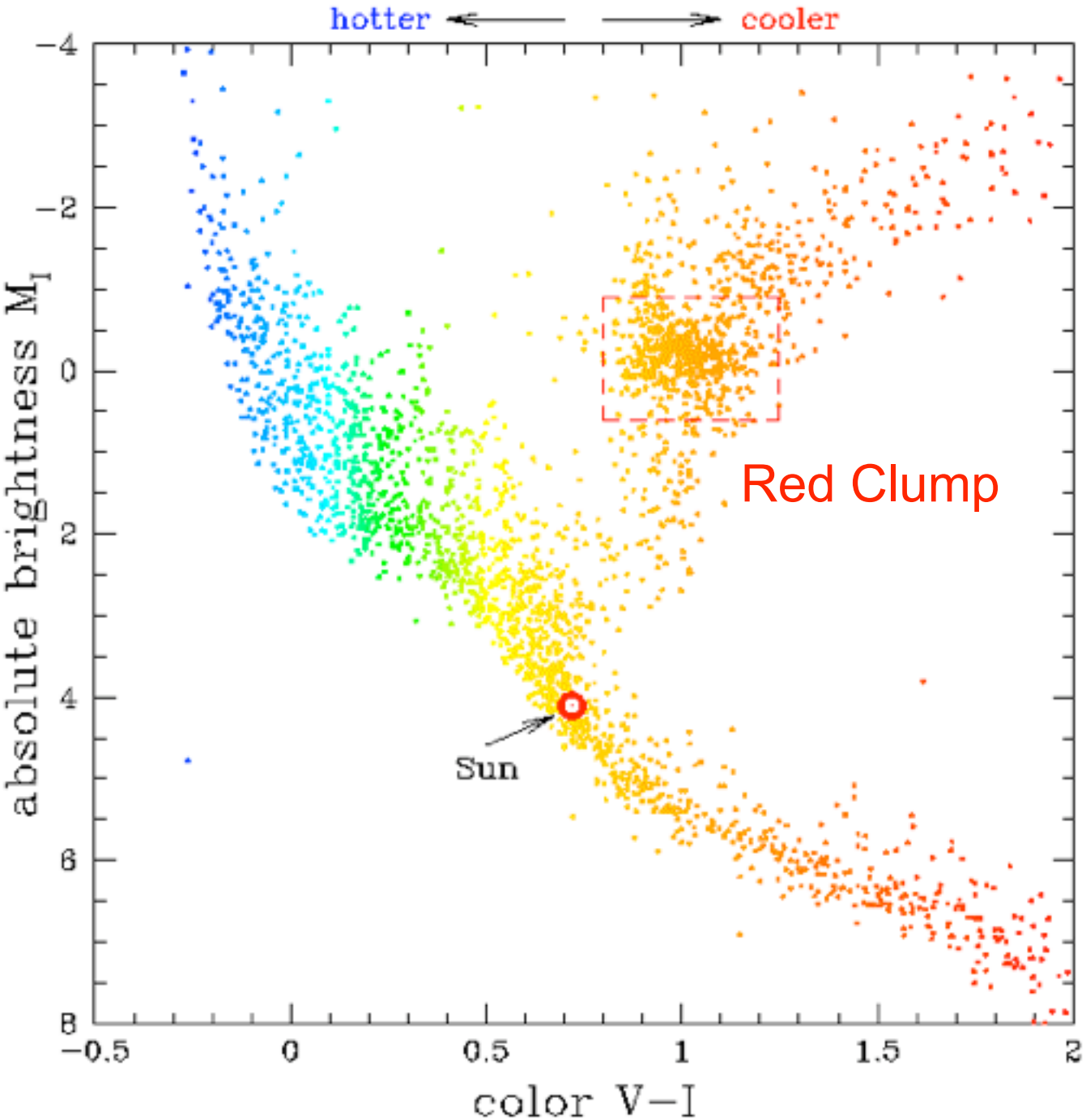

Secondary Distance Indicators

- Tully-Fisher relation
- Faber-Jackson relation
- Fundamental plane
- Type Ia supernovae
- Surface brightness fluctuations
- Extragalactic water masers

Extragalactic water masers

A geometric distance to the galaxy NGC4258 from orbital motions in a nuclear gas disk

J. R. Herrnstein et al. 1999, Nature, 400, 539. Dist to NGC4258 = 7.2±0.3 Mpc.

The distance is found by measuring the time-varying Doppler shift and proper motion around the central black hole. The Doppler shift is maximum when an object is moving along the l.o.s. and the proper motion is maximum when the object is moving perpendicular to the l.o.s.

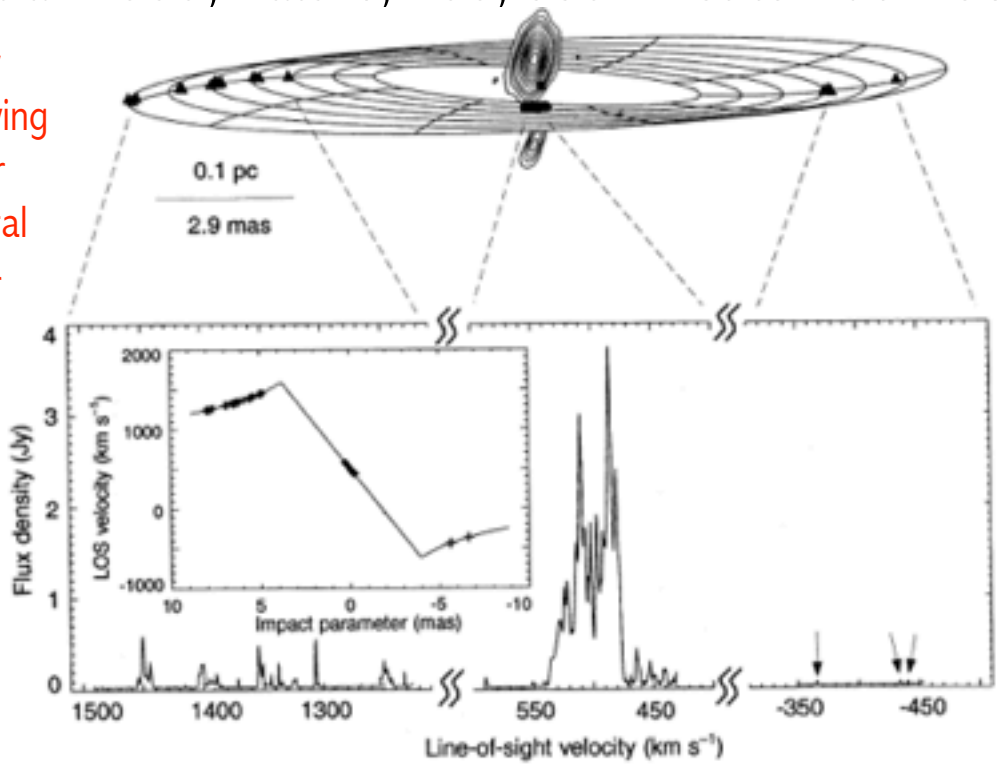

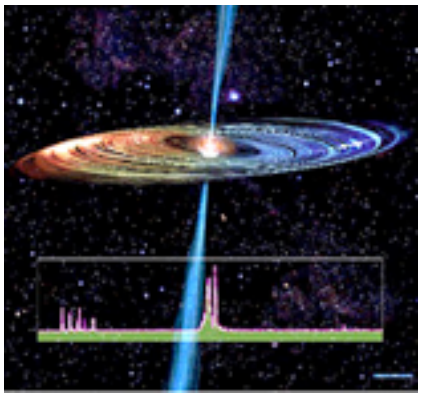

Artist's Conception

$M_{BH} = 3.9 \pm 0.1\ M_{sun}$

Figure 1 The NGC4258 water maser. The upper panel shows the best-fitting warped-disk model superposed on actual maser positions as measured by the VLBA of the NRAO, with top as North. The filled square marks the centre of the disk, as determined from a global disk-fitting analysis[8]. The filled triangles show the positions of the high-velocity masers, so called because they occur at frequencies corresponding to Doppler shifts of ~±1,000 km s^{-1} with respect to the galaxy systemic velocity of ~470 km s^{-1}. This is apparent in the VLBA total power spectrum (lower panel). The inset shows line-of-sight (LOS) velocity versus impact parameter for the best-fitting keplerian disk, with the maser data superposed. The high-velocity masers trace a keplerian curve to better than 1%. Monitoring of these features indicates that they drift by less than ~1 km s^{-1} yr^{-1} (refs 14–16) and requires that they lie within 5–10° of the midline, the intersection of the disk with the plane of the sky. The LOS velocities of the systemic masers are centred about the systemic velocity of the galaxy. The positions (filled circles in upper panel) and LOS velocities of these masers imply that they subtend ~8° of disk azimuth centred about the LOS to the central mass, and the observed acceleration (8–10 km s^{-1} yr^{-1}) of these features[14,15] unambiguously places them along the near edge of the disk. The approximately linear relationship between systemic maser impact parameter and LOS velocity demonstrates that the disk is very thin[17] (aspect ratio ≤ 0.2%) and that these masers are confined to a narrow annulus in the disk. The magnitude of the velocity gradient (Ω_s) implies a mean systemic radius, (r_s), of 3.9 mas which, together with the positions of the high-velocity masers, constrains the disk inclination, i_s, to be ~82 ± 1° (90° for edge-on). Finally, VLBA continuum images[7,13] are included as contours in the upper panel. The 22-GHz radio emission traces a sub-parsec-scale jet elongated along the rotation axis of the disk and well-aligned with a luminous, kiloparsec-scale jet[18].

Extragalactic water masers

A geometric distance to the galaxy NGC4258 from orbital motions in a nuclear gas disk

J. R. Herrnstein et al. 1999, Nature, 400, 539. Dist to NGC4258 = 7.2±0.3 Mpc.

we conclude that $\langle \dot{v}_{\rm LOS} \rangle = 9.3 \pm 0.3\,{\rm km\,s^{-1}\,yr^{-1}}$ and $\langle \dot{\theta}_x \rangle = 31.5 \pm 1\,\mu{\rm as\,yr^{-1}}$, where these (and all subsequent) uncertainties are 1σ values.

To convert the maser proper motions and accelerations into a geometric distance, we express $\langle \dot{\theta}_x \rangle$ and $\langle \dot{v}_{\rm LOS} \rangle$ in terms of the distance and four disk parameters:

$$\langle \dot{\theta}_x \rangle = 31.5 \left[\frac{D_6}{7.2}\right]^{-1} \left[\frac{\Omega_s}{282}\right]^{1/3} \left[\frac{M_{7.2}}{3.9}\right]^{1/3} \left[\frac{\sin i_s}{\sin 82.3^\circ}\right]^{-1} \left[\frac{\cos \alpha_s}{\cos 80^\circ}\right] \mu{\rm as\,yr^{-1}} \quad (1)$$

and

$$\langle \dot{v}_{\rm LOS} \rangle = 9.2 \left[\frac{D_6}{7.2}\right]^{-1} \left[\frac{\Omega_s}{282}\right]^{4/3} \left[\frac{M_{7.2}}{3.9}\right]^{1/3} \left[\frac{\sin i_s}{\sin 82.3^\circ}\right]^{-1} {\rm km\,s^{-1}\,yr^{-1}} \quad (2)$$

Here D_6 is the distance in Mpc, α_s is the disk position angle (East of North) at $\langle r_s \rangle$, and $M_{7.2}$ is $M/D \sin^2 i_s$ as derived from the high-velocity rotation curve and evaluated at $D = 7.2$ Mpc and $i_s = 82.3^\circ$ (in units of $10^7\,M_\odot$). $\Omega_s \equiv (GM_{7.2}/\langle r_s \rangle^3)^{1/2}$ is the projected disk angular velocity at $\langle r_s \rangle$

Determining the Hubble constant H_0 using multiple calibrators

A 3% SOLUTION: DETERMINATION OF THE HUBBLE CONSTANT WITH THE *HUBBLE SPACE TELESCOPE* AND WIDE FIELD CAMERA 3*

Adam G. Riess et al. THE ASTROPHYSICAL JOURNAL, 730:119 (18pp), 2011 April 1

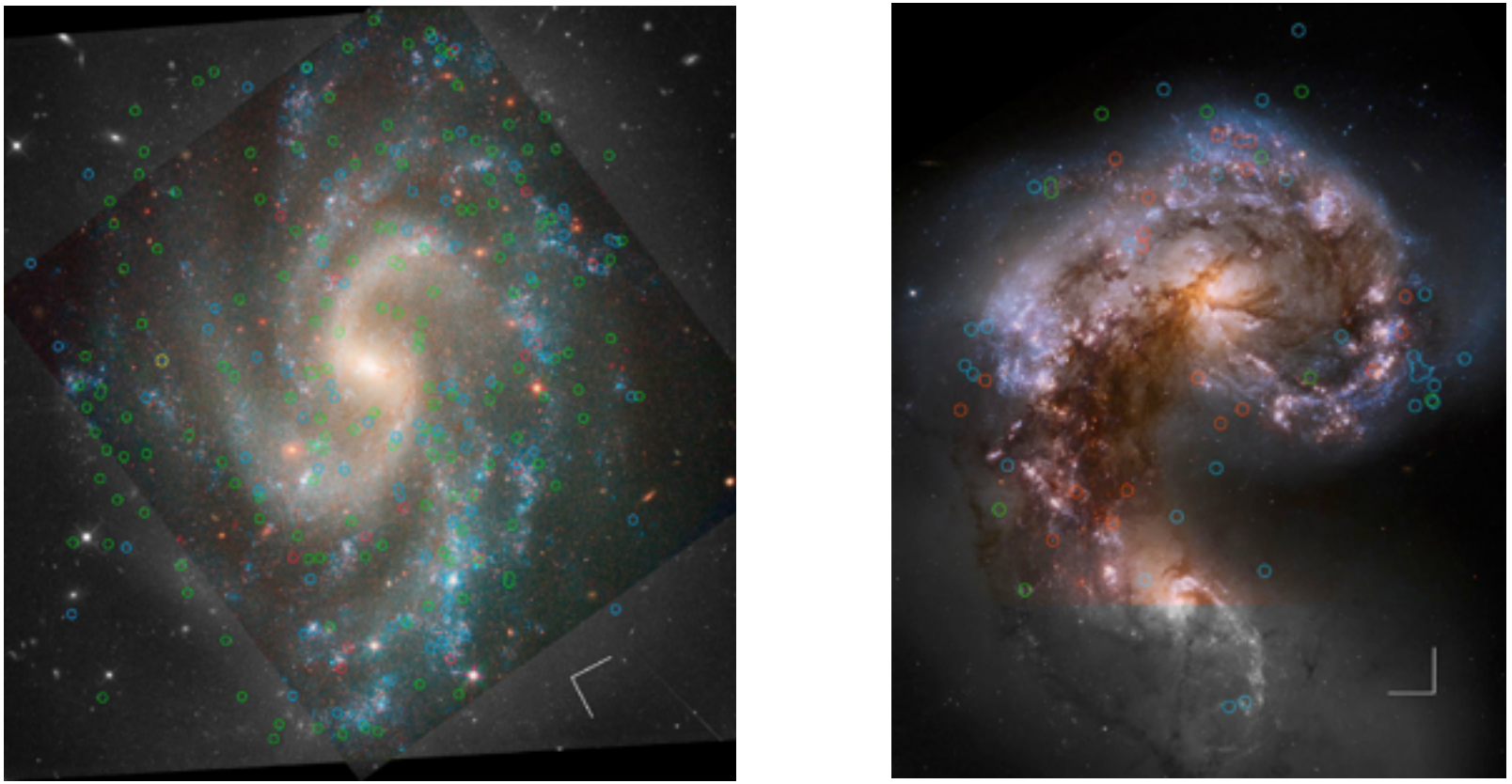

HST images of NGC 5584 and NGC 4038/9.. The positions of Cepheids with periods in the rangeP > 60 days, 30 days < P < 60 days, and 10 days < P < 30 days are indicated by red, blue, and green circles, respectively. A yellow circle indicates the position of the host galaxy's SN Ia. The orientation is indicated by the compass rose whose vectors have lengths of 15((and indicate north and east. The black and white regions of the images show the WFC3 optical data and the color includes the WFC3–IR data.

Determining the Hubble constant H_0 using multiple calibrators

A 3% SOLUTION: DETERMINATION OF THE HUBBLE CONSTANT WITH THE *HUBBLE SPACE TELESCOPE* AND WIDE FIELD CAMERA 3*

Adam G. Riess et al. THE ASTROPHYSICAL JOURNAL, 730:119 (18pp), 2011 April 1

$H_0 = 73.8 \pm 2.4$ km s^{-1} Mpc^{-1} including systematic errors, corresponding to a 3.3% uncertainty.

Figure 9. Uncertainties in the determination of the Hubble constant. Uncertainties are squared to show their contribution to the quadrature sum. These terms are given in Table 5.

Table 5
H_0 Error Budget for Cepheid and SN Ia Distance Ladders[a]

Term	Description	Previous LMC	R09 N4258	Here N4258	Here All Three[b]
σ_{anchor}	Anchor distance	5%	3%	3%	1.3%
$\sigma_{anchor-PL}$	Mean of P–L in anchor	2.5%	1.5%	1.4%	0.7%[c]
$\sigma_{host-PL}/\sqrt{n}$	Mean of P–L values in SN hosts	1.5%	1.5%	0.6 %	0.6%
$\sigma_{SN}/\sqrt{n}$	Mean of SN Ia calibrators	2.5%	2.5%	1.9%	1.9%
σ_{m-z}	SN Ia m–z relation	1%	0.5%	0.5%	0.5%
$R\sigma_{\lambda,1,2}$	Cepheid reddening, zero points, anchor-to-hosts	4.5%	0.3%	0.0%	1.4%
σ_Z	Cepheid metallicity, anchor-to-hosts	3%	1.1%	0.6 %	1.0%
σ_{PL}	P–L slope, $\Delta\log P$, anchor-to-hosts	4%	0.5%	0.4%	0.6%
σ_{WFPC2}	WFPC2 CTE, long-short	3%	0%	0%	0%
Subtotal, σ_{H_0}		10%	4.7 %	4.0%	2.9%
Analysis systematics		NA	1.3%	1.0%	1.0%
Total, σ_{H_0}		10%	4.8 %	4.1%	3.1%

Notes.
[a] Derived from diagonal elements of the covariance matrix propagated via the error matrices associated with Equations (1), (3), (7), and (8).
[b] Using the combination of all three calibrations of the Cepheid distance scale, LMC, MW parallaxes, and NGC 4258.
[c] For MW parallax, this term is already included with the term above.

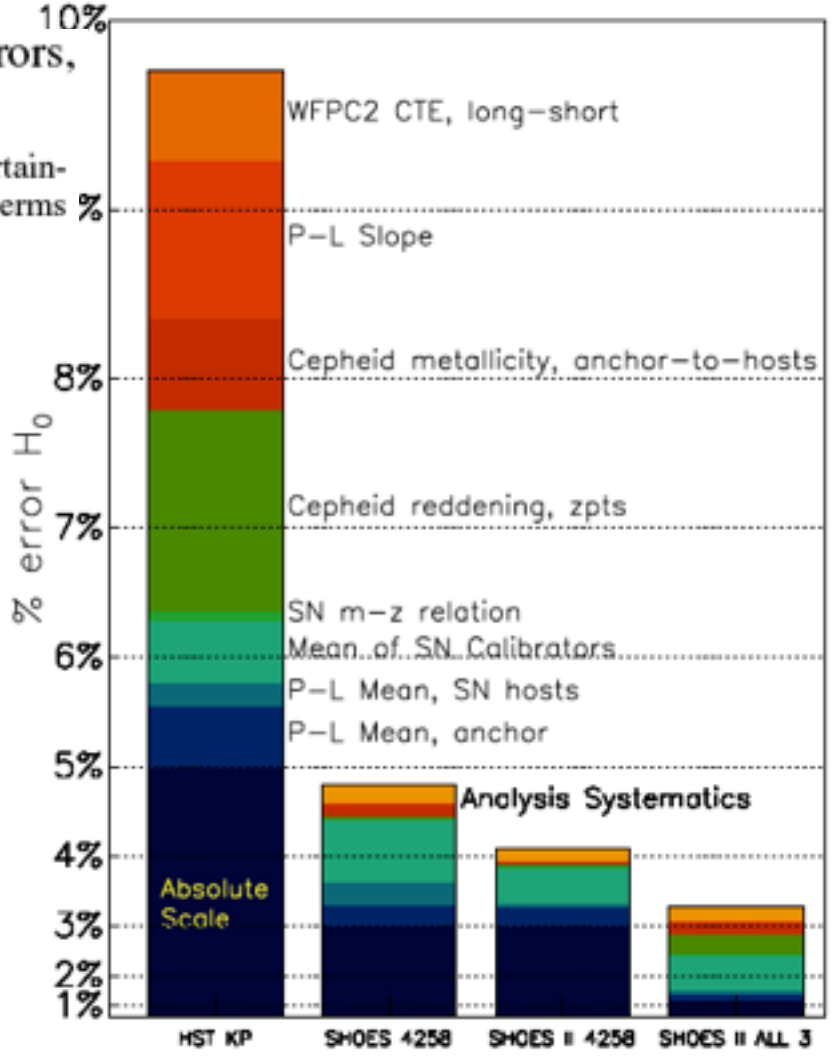

The Age of the Universe

In the mid-1990s there was a crisis in cosmology, because the age of the old Globular Cluster stars in the Milky Way, then estimated to be 16±3 Gyr, was higher than the expansion age of the universe, which for a critical density ($\Omega_m = 1$) universe is 9±2 Gyr (with the Hubble parameter h=0.72±0.07).

But when the data from the Hipparcos astrometric satellite became available in 1997, it showed that the distance to the Globular Clusters had been under-estimated, which implied that their ages are 12±3 Gyr.

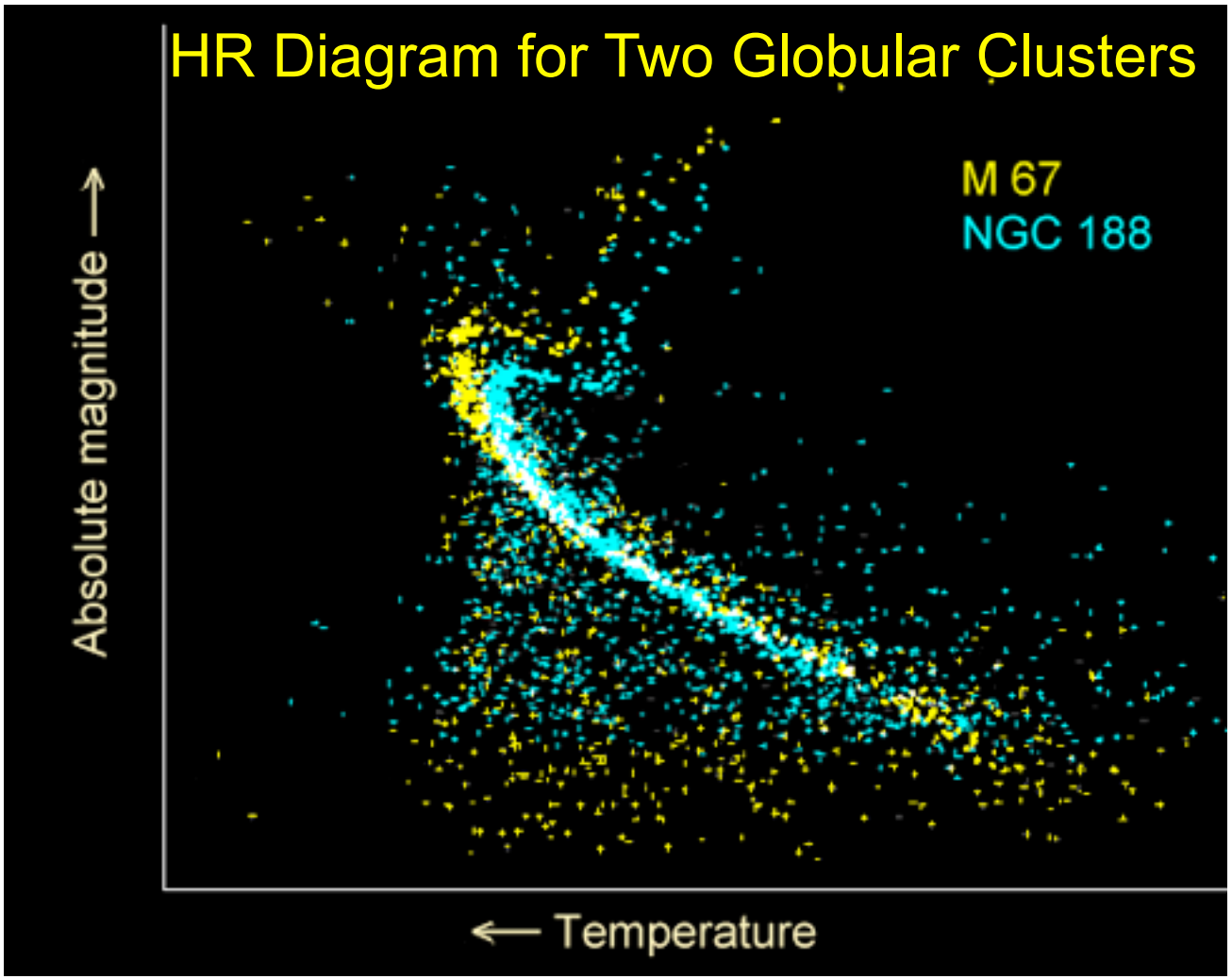

The Age of the Universe

In the mid-1990s there was a crisis in cosmology, because the age of the old Globular Cluster stars in the Milky Way, then estimated to be 16±3 Gyr, was higher than the expansion age of the universe, which for a critical density ($\Omega_m = 1$) universe is 9±2 Gyr (with the Hubble parameter h=0.72±0.07). But when the data from the Hipparcos astrometric satellite became available in 1997, it showed that the distance to the Globular Clusters had been underestimated, which implied that their ages are 12±3 Gyr.

Several lines of evidence now show that the universe does not have $\Omega_m = 1$ but rather $\Omega_{tot} = \Omega_m + \Omega_\Lambda = 1.0$ with $\Omega_m \approx 0.3$, which gives an expansion age of about 14 Gyr.

Moreover, a new type of age measurement based on radioactive decay of Thorium-232 (half-life 14.1 Gyr) measured in a number of stars gives a completely independent age of 14±3 Gyr. A similar measurement, based on the first detection in a star of Uranium-238 (half-life 4.47 Gyr), gives 12.5±3 Gyr.

All the recent measurements of the age of the universe are thus in excellent agreement. It is reassuring that three completely different clocks – stellar evolution, expansion of the universe, and radioactive decay – agree so well.

Age of the Universe t_0 in FRW Cosmologies

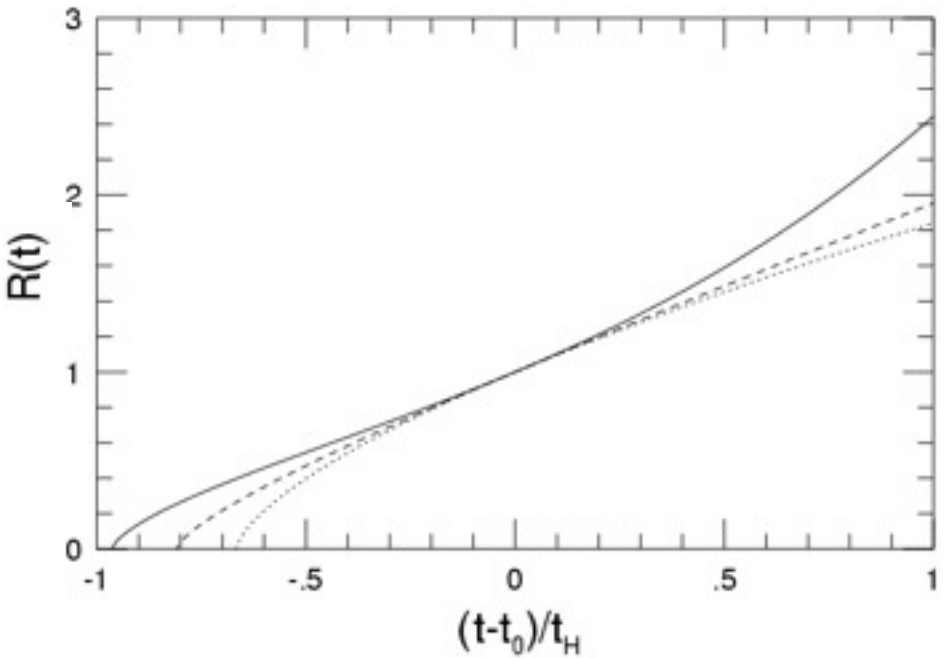

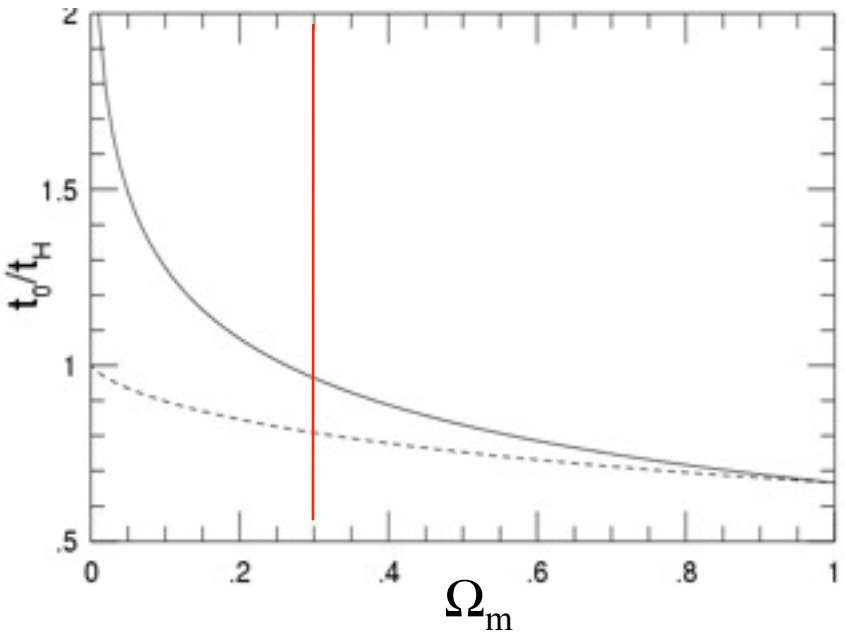

(a) Evolution of the scale factor $a(t)$ plotted vs. the time after the present $(t - t_0)$ in units of Hubble time $t_H \equiv H_0^{-1} = 9.78h^{-1}$ Gyr for three different cosmologies: Einstein-de Sitter ($\Omega_0 = 1, \Omega_\Lambda = 0$ dotted curve), negative curvature ($\Omega_0 = 0.3, \Omega_\Lambda = 0$: dashed curve), and low-Ω_0 flat ($\Omega_0 = 0.3$, $\Omega_\Lambda = 0.7$: solid curve). (b) Age of the universe today t_0 in units of Hubble time t_H as a function of Ω_0 for $\Lambda = 0$ (dashed curve) and flat $\Omega_0 + \Omega_\Lambda = 1$ (solid curve) cosmologies.

Evolution of Densities of Radiation, Matter, & Λ

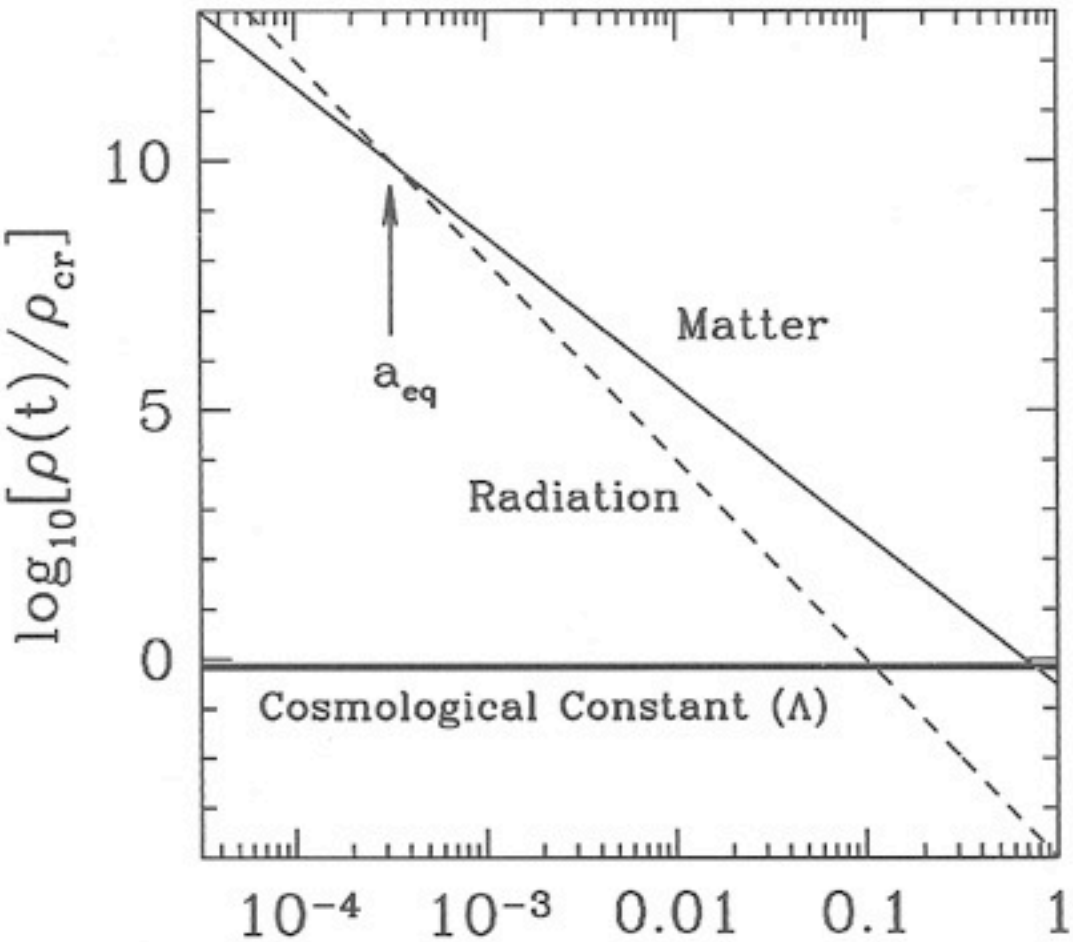

Figure 1.3. Energy density vs scale factor for different constituents of a flat universe. Shown are nonrelativistic matter, radiation, and a cosmological constant. All are in units of the critical density today. Even though matter and cosmological constant dominate today, at early times, the radiation density was largest. The epoch at which matter and radiation are equal is a_{eq}.

Dodelson, Chapter 1

History of Cosmic Expansion for General Ω_M & Ω_Λ

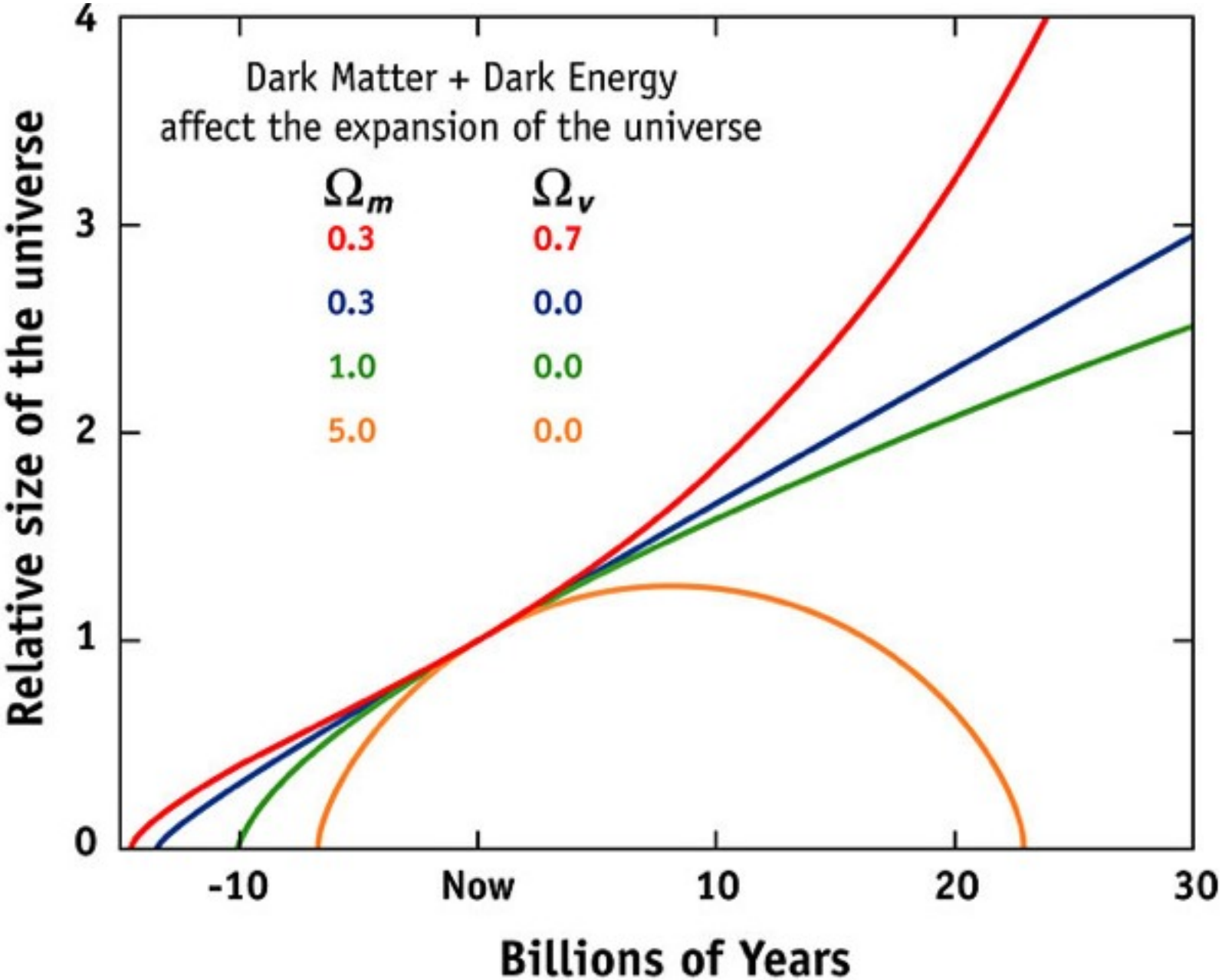

History of Cosmic Expansion for $\Omega_\Lambda = 1 - \Omega_M$

With Ω_Λ = 0 the age of the decelerating universe would be only 9 Gyr, but Ω_Λ = 0.7, Ω_m = 0.3 gives an age of 14Gyr, consistent with stellar and radioactive decay ages

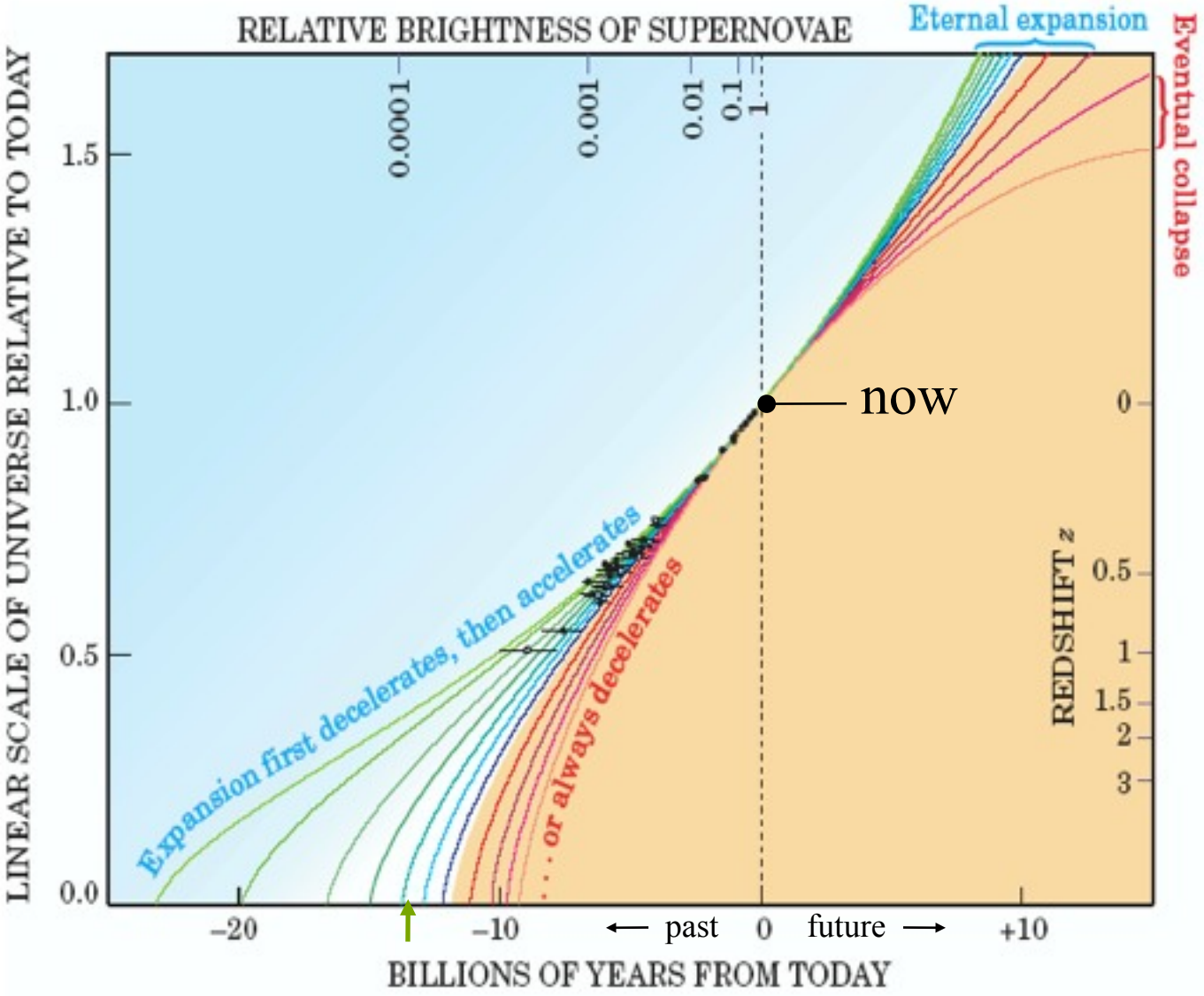

Figure 4. The history of cosmic expansion, as measured by the high-redshift supernovae (the black data points), assuming flat cosmic geometry. The scale factor R of the universe is taken to be 1 at present, so it equals $1/(1 + z)$. The curves in the blue shaded region represent cosmological models in which the accelerating effect of vacuum energy eventually overcomes the decelerating effect of the mass density. These curves assume vacuum energy densities ranging from 0.95 ρ_c (top curve) down to 0.4 ρ_c. In the yellow shaded region, the curves represent models in which the cosmic expansion is always decelerating due to high mass density. They assume mass densities ranging (left to right) from 0.8 ρ_c up to 1.4 ρ_c. In fact, for the last two curves, the expansion eventually halts and reverses into a cosmic collapse.

Saul Perlmutter, *Physics Today*, Apr 2003

Brief History of the Universe

- Cosmic Inflation generates density fluctuations
- Symmetry breaking: more matter than antimatter
- All antimatter annihilates with almost all the matter (1s)
- Big Bang Nucleosynthesis makes light nuclei (10 min)
- Electrons and light nuclei combine to form atoms, and the cosmic background radiation fills the newly transparent universe (380,000 yr)

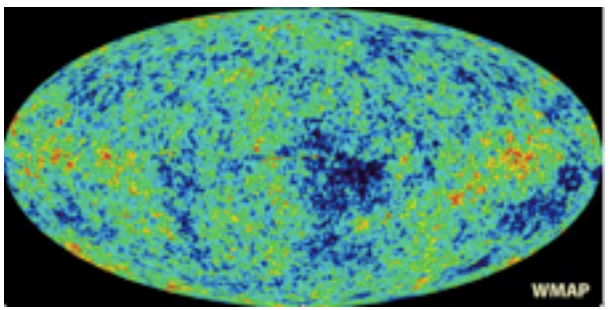

- Galaxies and larger structures form (~1 Gyr)
- Carbon, oxygen, iron, ... are made in stars
- Earth-like planets form around 2nd generation stars
- Life somehow starts (~4 Gyr ago) and evolves on earth

Mapping the large scale structure of the universe ...

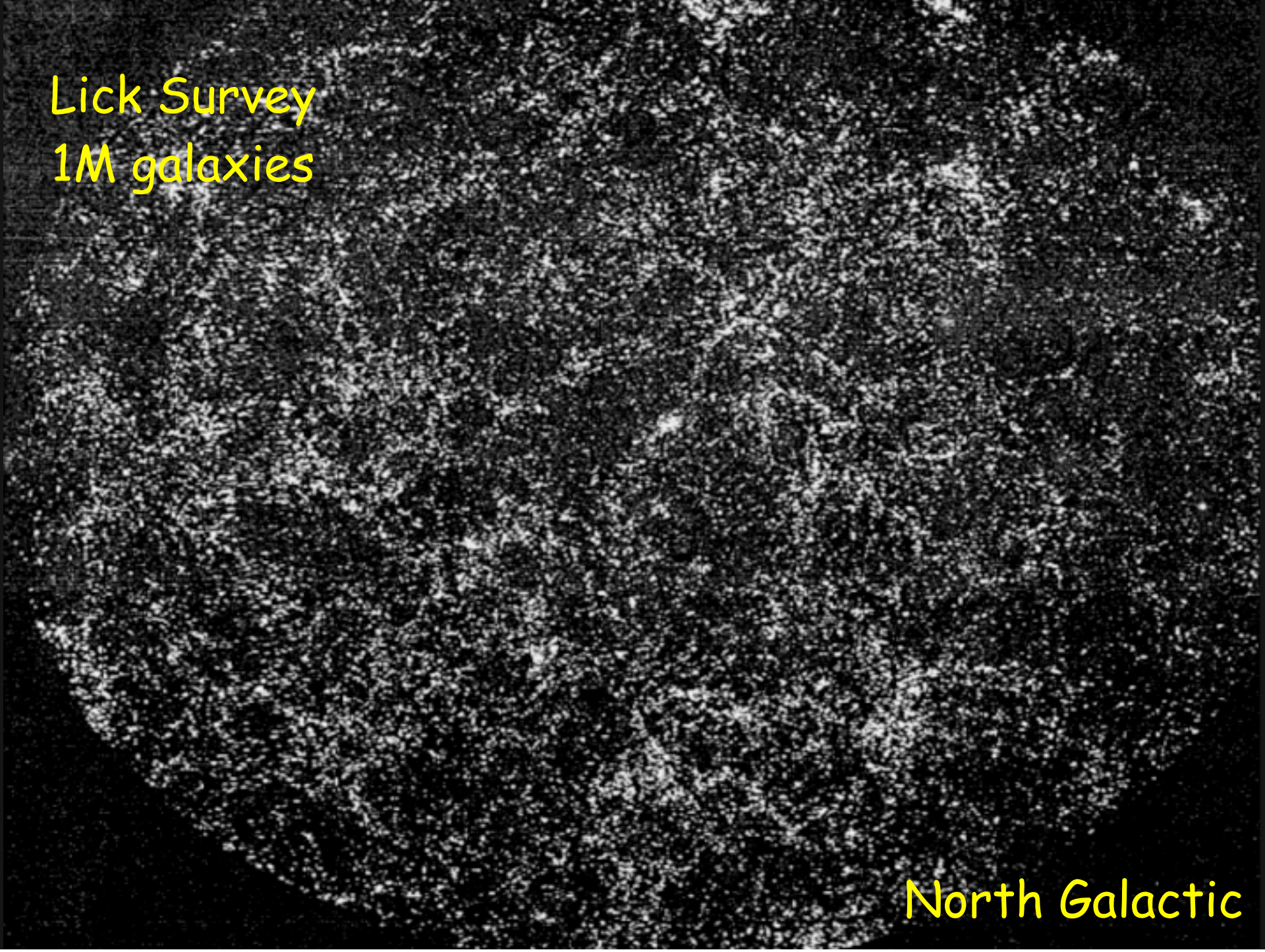
Lick Survey
1M galaxies
North Galactic

CfA survey: Great Wall

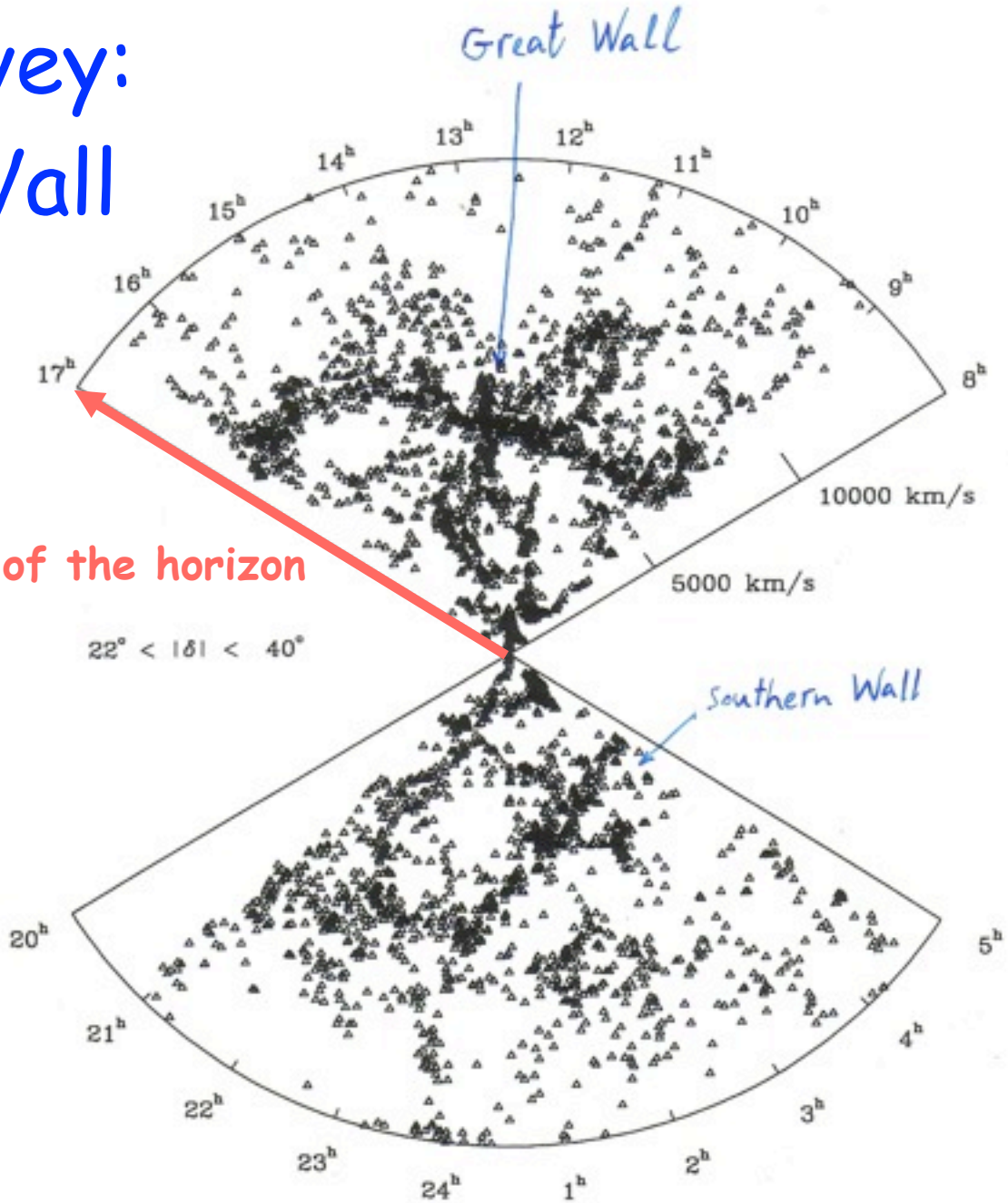

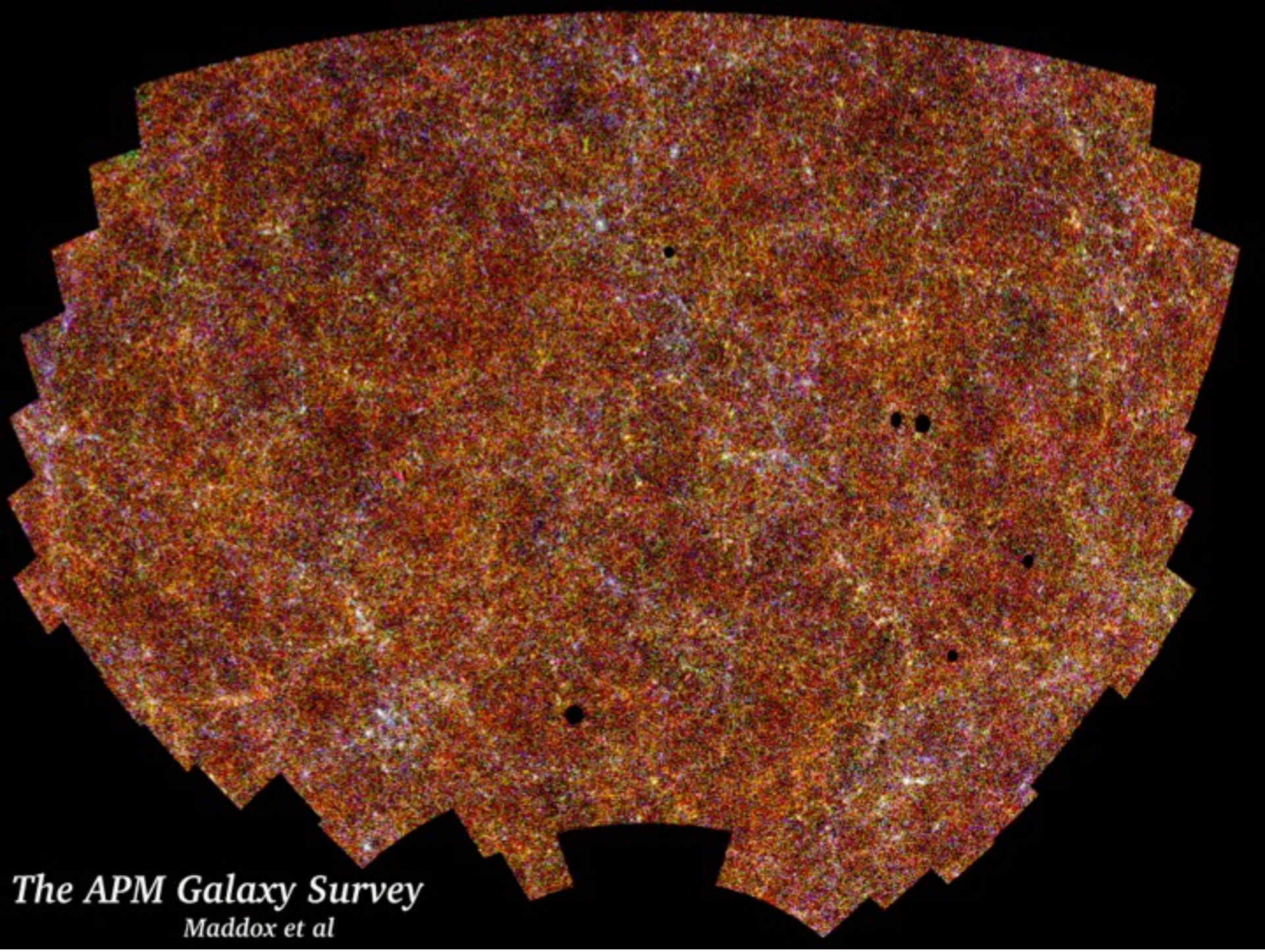
The APM Galaxy Survey
Maddox et al

2dF Galaxy Redshift Survey

¼ M galaxies 2003

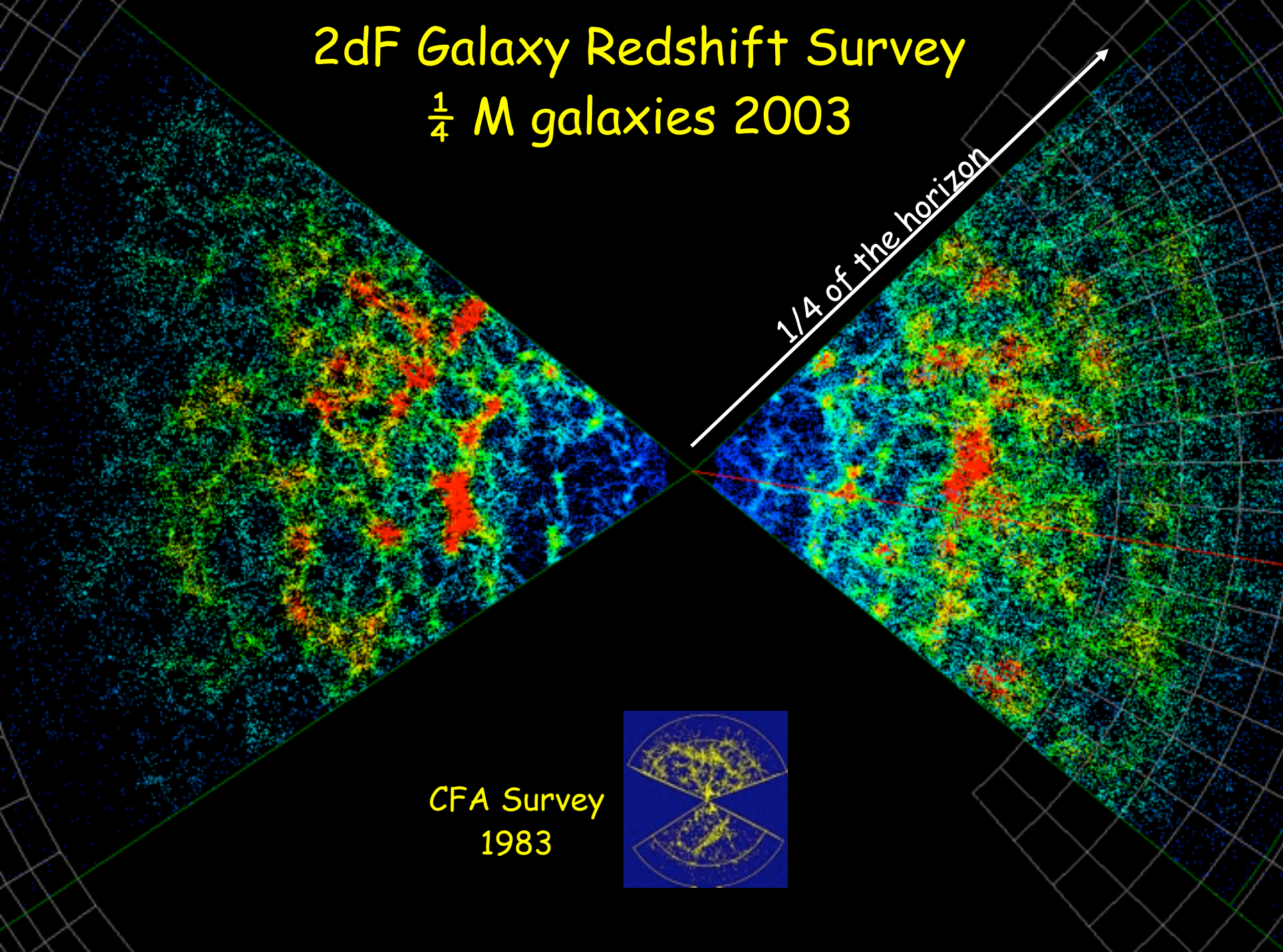

CFA Survey
1983

Mapping the Galaxies
Sloan Digital Sky Survey

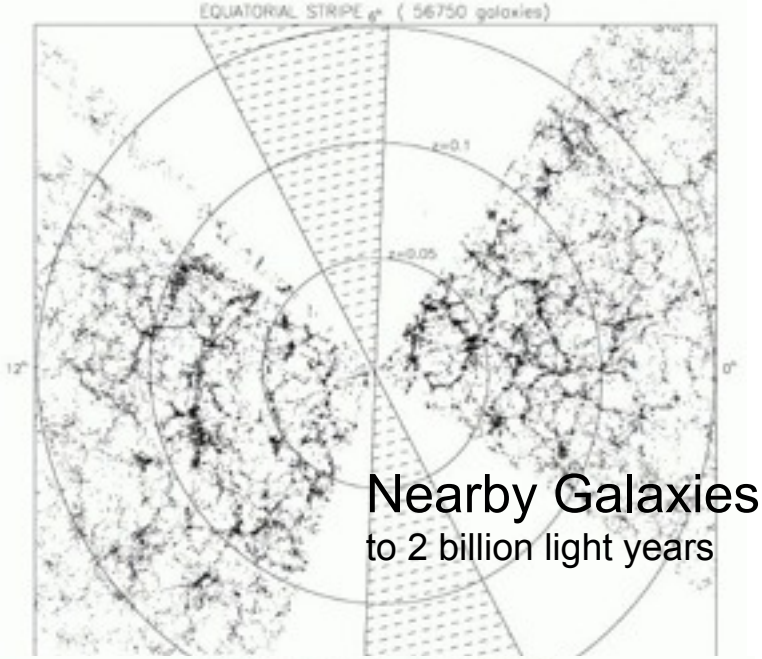

Nearby Galaxies
to 2 billion light years

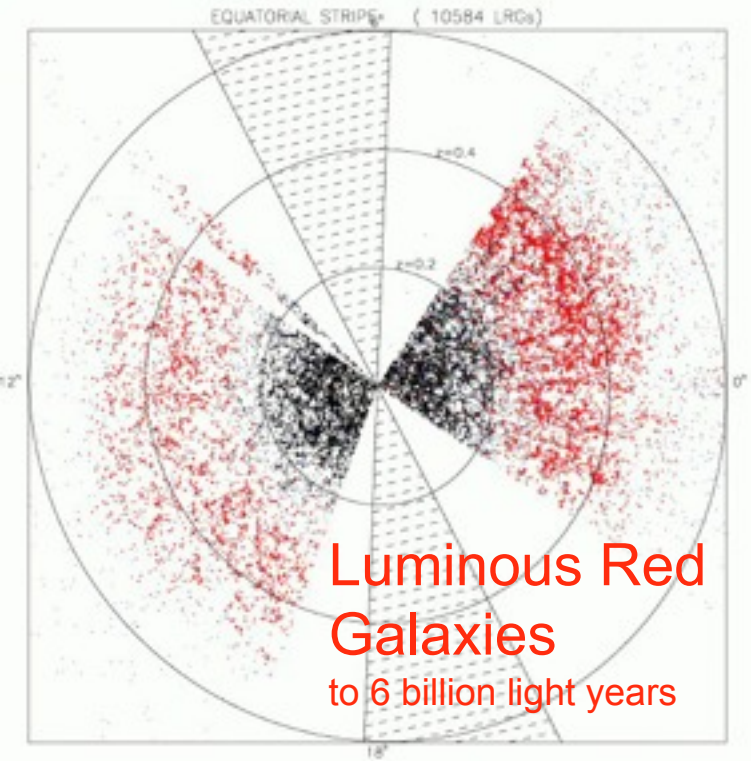

Luminous Red Galaxies
to 6 billion light years

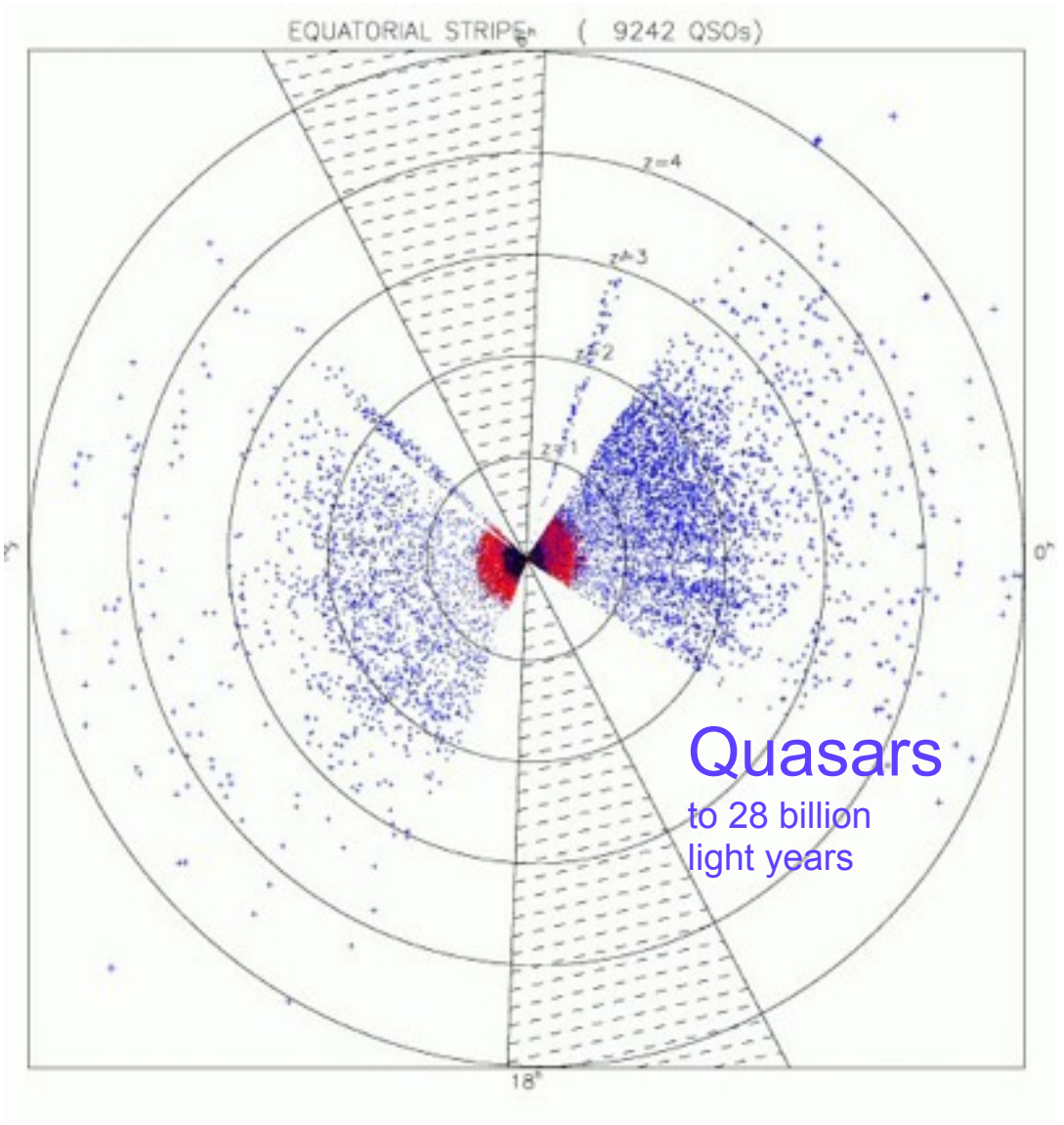

Quasars
to 28 billion light years

GALAXIES MAPPED BY THE SLOAN SURVEY

Data Release 4:
565,715 Galaxies & 76,403 Quasars

GALAXIES MAPPED BY THE SLOAN SURVEY

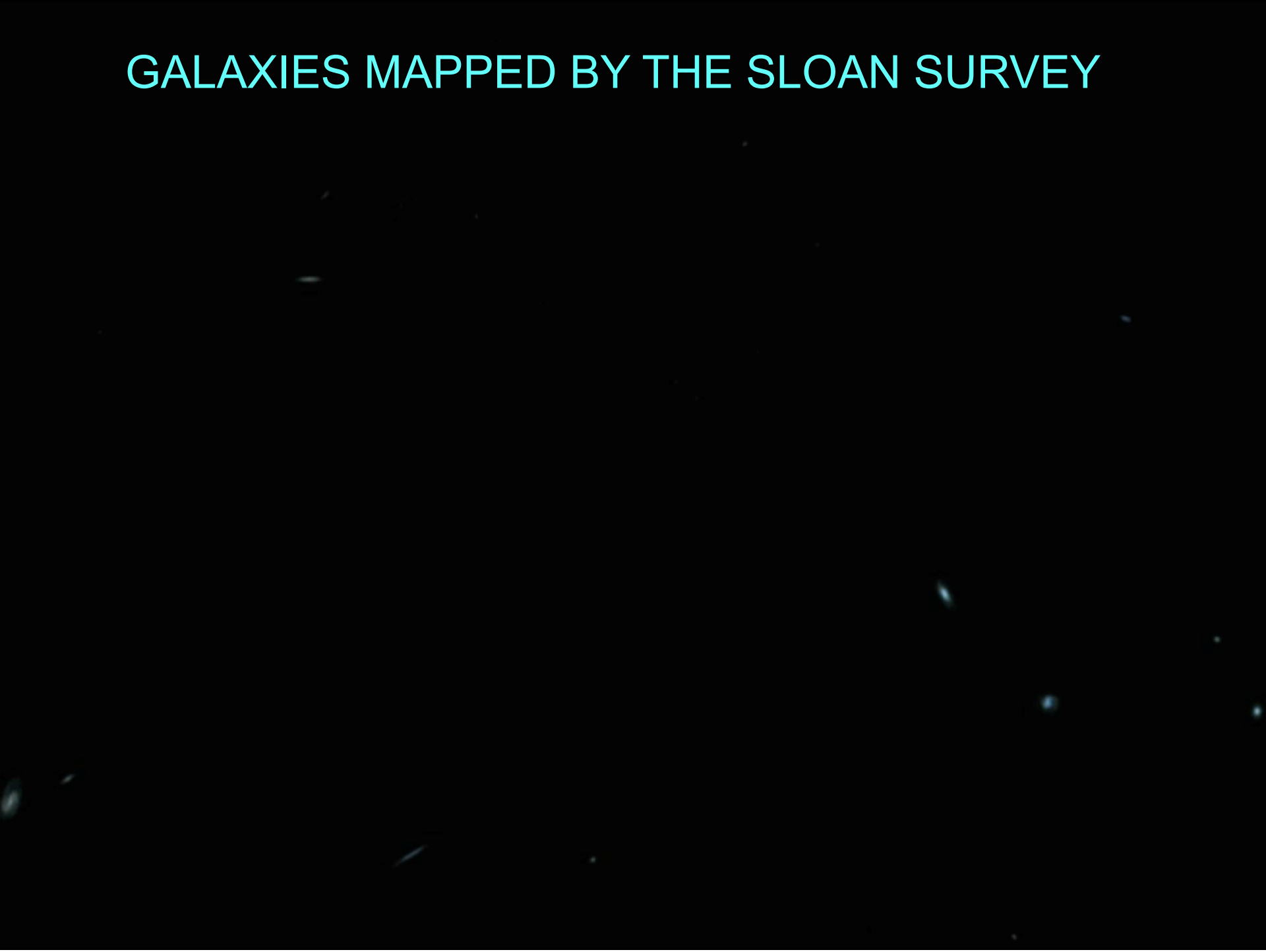

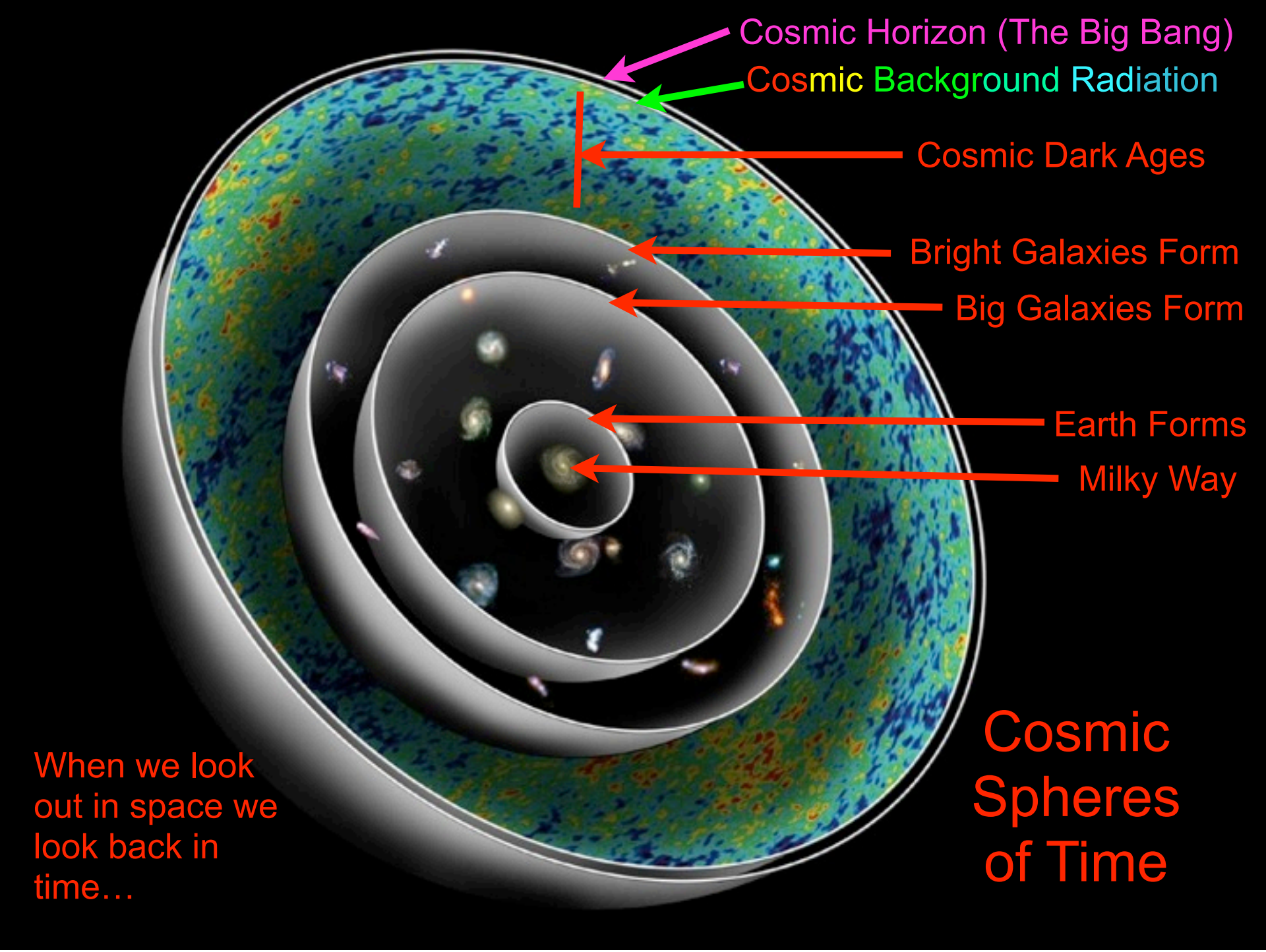
Cosmic Horizon (The Big Bang)
Cosmic Background Radiation
Cosmic Dark Ages
Bright Galaxies Form
Big Galaxies Form
Earth Forms
Milky Way
When we look out in space we look back in time…
Cosmic Spheres of Time

Medieval Universe

The geocentric pre-Copernican Universe in Christian Europe. At center, Earth is divided into Heaven (tan) and Hell (brown). The elements water (green), air (blue) and fire (red) surround the Earth. Moving outward, concentrically, are the spheres containing the seven planets, the Moon and the Sun, as well as the "Twelve Orders of the Blessed Spirits," the Cherubim and the Seraphim. German manuscript, c. 1450.